Power smoothing by kite tether force control for megawatt-scale airborne wind energy systems

Hummel, J.I.S.; Pollack, T.S.C.; Eijkelhof, D.; van Kampen, E.; Schmehl, R.

DOI
10.1088/1742-6596/2767/7/072019

Publication date
2024

Document Version
Final published version

Published in
Journal of Physics: Conference Series

Power smoothing by kite tether force control for megawatt-scale airborne wind energy systems

Journal of Physics: Conference Series **2767** (2024) 072019 doi:10.1088/1742-6596/2767/7/072019

Power smoothing by kite tether force control for megawatt-scale airborne wind energy systems

JIS Hummel, TSC Pollack, D Eijkelhof, E van Kampen and R Schmehl

Faculty of Aerospace Engineering, Delft University of Technology, 2629 HS Delft, The Netherlands.

E-mail: j.i.s.hummel@tudelft.nl

Abstract. Airborne wind energy is an emerging technology that uses tethered flying devices to capture stronger and more steady winds at higher altitudes. Compared to smaller systems, megawatt-scale systems are substantially affected by gravity during flight operation, resulting in power fluctuations. MegAWES, a 3 MW reference model, experiences power fluctuations between -5.8 MW and +20.5 MW every 12.5 seconds during the traction phase when using its baseline controller at a wind speed of 22 m/s. The baseline controller does not have a power limit, leading to high peak power, and aims to keep the tether force constant, causing it to consume power when the kite is flying upwards. In this paper, we implement an optimal torque controller in the MegAWES framework and show that this eliminates the power consumption during the traction phase. Furthermore, we propose a kite tether force controller that allows setting a power limit when combined with the 2-phase reeling strategy, which decreases the peak power. Our new architecture reduces the power output range by 75% to between +3.7 MW and +9.4 MW in strong wind conditions.

1. Introduction

Airborne wind energy (AWE) is a promising technology that aims to reach the stronger and more steady high altitude winds by using tethered flying devices [1]. Loyd [2] first envisioned this concept, estimating a potential to extract multi-megawatts of power from high altitude winds. The flying devices, tethered to a ground station, follow circular or figure-eight patterns mostly perpendicular to the wind. Four prevalent system concepts are illustrated in Fig. 1 [3].

This study focuses on the fixed-wing with ground-generation concept, which utilizes rigid materials for the kite and generates power at a ground-based station. The system operates in two phases: traction (energy-generating) and retraction (energy-consuming). In the traction phase, the kite's pull on the tether is converted into electricity by rotating the ground-based winch and generator. During retraction, the system, with the kite placed in an aerodynamically favorable position, consumes only a fraction of the energy produced in the traction phase [1].

The rated power of systems currently in development ranges from 1 kW to 200 kW [4]. However, they should be scaled up to megawatt-scale to achieve utility power production [5]. "MegAWES" is the first publicly available multi-megawatt, ground-gen, fixed-wing reference model and simulation framework [6, 7]. It has a nominal power output of 3.0 MW and is intended for cross-validation and benchmarking. MegAWES utilizes a control architecture adapted from [8], which uses the winch to keep the tether force constant during the traction phase. While

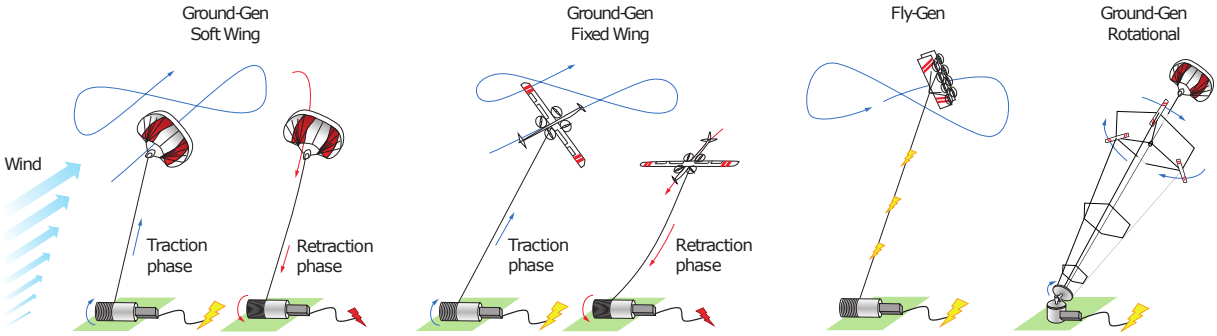

Figure 1: Illustration of the four most advanced airborne wind energy system concepts. From left to right: soft wing with ground-gen, fixed-wing with ground-gen, fixed-wing with fly-gen, and the rotating kite concept. Figure obtained from [3].

effective in preventing tether rupture, this approach leads to significant power fluctuations [8] and cannot take a power limit into account. Computational simulations of MegAWES with the point-mass aircraft model at a wind speed of 22 m/s result in power fluctuations between 20.5 MW and −5.8 MW during the traction phase. Note that the system momentarily has to consume power to keep the tether force constant when the kite is flying upwards and opposing gravity. When flying downwards, the kite's pull is increased because of gravitational effects and the system has to reel-out fast to keep the tether force constant, leading to a high peak power. These power fluctuations require smoothing as a necessary step before transmission to the energy grid [9]. Larger fluctuations thus require over-dimensioning of components, increasing system cost. In particular the generator, which is sized for the peak load, which occurs most frequently at high wind speeds.

Instead of keeping a constant tether force, most winch controllers aim to follow the optimal reel-out speed for power production [10, 11, 12, 13]. This is analogous to optimal torque control for wind turbines, which aims to rotate the rotor to track the optimal tip speed ratio [14]. These controllers allow a varying tether force based on the pull of the kite but have not been tested yet on megawatt-scale systems with significant mass to evaluate their effect on power fluctuations.

Besides increasing the minimum power, the peak power should be reduced to avoid overloading the generator. In wind turbines, this is done by collective pitch control above rated wind speed, by pitching the blade to decrease the lift-to-drag ratio and limit energy capture from the wind [14]. Similarly, for kites, aerodynamic performance can be reduced by changing the angle of attack. Numerous optimal control studies compute a dynamic angle of attack reference [15, 16] or use flight controllers that follow a precomputed angle of attack reference [17, 18]. However, these studies focus on system analysis or trajectory optimization and lack practical implementation outside simulation due to unaccounted model uncertainties and/or hardware constraints.

This work aims to reduce power fluctuations in megawatt-scale airborne wind energy systems in strong wind conditions through two contributions to the MegAWES simulation framework:

(i) Implementation of an optimal torque controller. This allows a lower tether force when flying upwards, thus increasing the minimum power.

(ii) Formulation and implementation of kite tether force control. It is used in conjunction with the 2-phase strategy where the tether force limit and power limit are reached at the same reel-out speed [19]. By then regulating the tether force using the angle of attack, the control architecture can take a power limit into account, thus reducing the peak power.

The paper proceeds as follows: Section 2 describes the MegAWES simulation framework,

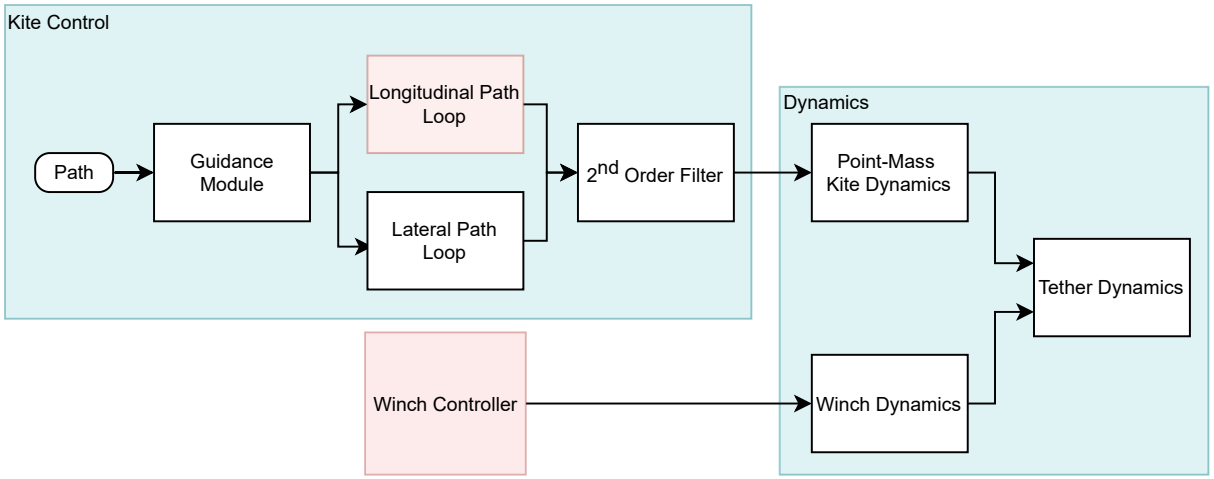

Figure 2: Block diagram (feedback paths are omitted) of the traction-phase controller for the point-mass dynamics, as proposed by [6], based on [8] and referred to as the "baseline" controller in this work. The winch controller and longitudinal path loop, indicated in red, are replaced in this work by an optimal torque winch controller and the kite tether force controller.

including the baseline control architecture. Section 3 outlines the proposed control architecture, integrating optimal torque control with the proposed kite tether force controller. Section 4 presents and discusses performance differences between the different control architectures. The paper concludes in Section 5.

2. MegAWES model and baseline controller description

In this section, the setup in the MegAWES simulation framework and the baseline control architecture is presented. The MegAWES reference design is presented in detail in [6] and the GitHub repository for the simulation framework can be found at [7].

2.1. Model Setup

The MegAWES simulation framework features different fidelity levels. In this work, the point-mass dynamics are used. The angle of attack can then be directly commanded, in contrast to commanding the elevators in the 6DOF dynamics. This allows a focus on the core of the kite tether force control concept: an angle of attack reference controller.

2.2. Control Architecture

The block diagram with the kite controller, winch controller, and dynamics is given in Fig. 2, with indications which parts will be changed in this work. As mentioned in Section 1, this cascaded control architecture is based on [8] and adapted for the MegAWES system. Section 4 will use this control architecture as a baseline for comparison to our controllers.

The reference path is a continuous figure of eight and the Guidance Module sets the reference course and path angle rates that should drive the kite towards that path. In the Path Loop, the kite controller assumes that the winch keeps the tether force at a constant reference value. Since the gravity force is known, the controller can solve the required aerodynamic force to stay on the path, which is then used to set the reference bank angle and angle of attack. In the point-mass dynamics, the bank angle and angle of attack can be directly set, so to mimic the

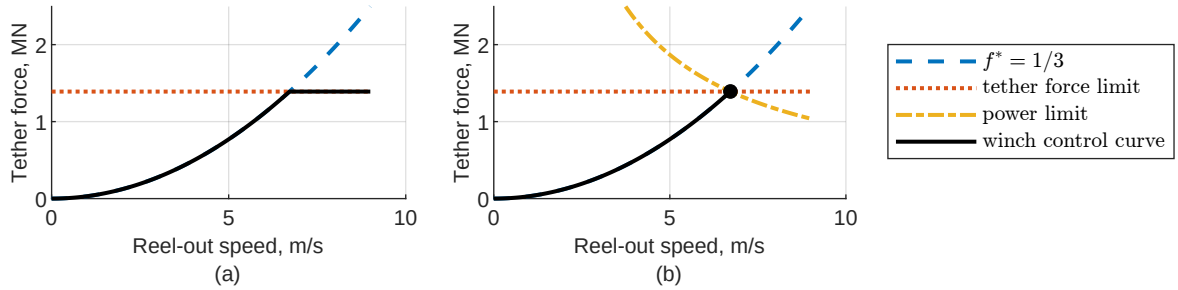

Figure 3: Winch control curves for the two control strategies. The optimal torque control strategy (a) follows the optimal reel-out factor until the tether force limit is reached and then aims to keep the tether force constant. The kite tether force control strategy (b) follows the optimal reel-out factor until the tether force and power limit are reached and then aims to stay at those limits by using kite tether force control.

response delay that would be present in a 6DOF simulation, where the inner loop controller uses the control deflectors to follow the reference attitude, a second-order filter is added.

The baseline winch controller follows a constant tether force reference for a given wind speed using a PI controller. This work will change this winch controller to an optimal torque controller.

In our simulations, we use the inertia and radius for the winch that we propose in [20]. The winch size proposed by [6] is based on a smaller system and has very high frequency dynamics, making the system unrealistic and resulting in poor performance. By increasing the inertia and radius of the winch, the simulation is more realistic and the winch controller performs better.

3. Optimal torque control and kite tether force control

In this section, two control architectures are presented. First, the optimal torque controller is discussed, and a tether force limit is added. Then, the kite tether force controller is formulated which enables a power limit. The code for both controllers can be found at [21].

3.1. Optimal torque control

The winch control law uses a feedback strategy that aims to maximize energy capture by keeping the system at the optimal reel-out factor f^*, where $f = v_\mathrm{r}/v_\mathrm{w}$, where v_r denotes the reel-out speed and v_w the wind speed.This is analogous to wind turbines operating at their optimal tip-speed ratio [14]. Determining the optimal reel-out factor for MegAWES is not the focus of this study, so a reel-out factor of $f^* = 1/3$ [2] is assumed. The control law can then be derived by assuming steady-state reeling of a massless system and setting the torque such that the system achieves an equilibrium at the optimal reel-out factor; see [10]:

$$\tau = 4\mathscr{C} v_\mathrm{r}^2 r, \quad \mathscr{C} = \frac{1}{2}\rho S C_\mathrm{L} E_\mathrm{eq}^2 \left(1 + \frac{1}{E_\mathrm{eq}}\right)^{\frac{3}{2}}, \tag{1}$$

where τ denotes the winch control torque, ρ the air density, S the reference wind area, C_L the lift coefficient, E_eq the equivalent lift-to-drag ratio (taking the tether drag into account). The constant $\mathscr{C}$ is related to the performance and size of the kite.

By dividing the optimal torque by the radius of the winch, the optimal tether force for a given reel-out speed was calculated. This is shown with the label $f^* = 1/3$ in Fig. 3. By adding a tether force limit, the strategy for the the optimal torque controller is shown in the left plot in Fig. 3. So the winch controller consists of a control law that aims to reel-out the system at the optimal reel-out factor (Eq. (1)), and a part that limits the peak tether force. In this work,

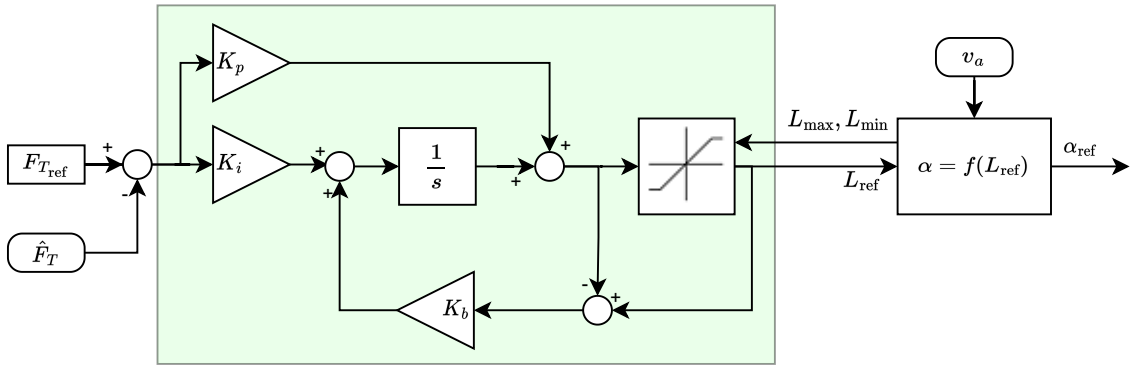

Figure 4: Block diagram of the kite tether force controller. From the tether force error a PI controller with anti-windup outputs a reference lift force that is then converted to a reference angle of attack by inverting the linear lift curve. The safe bounds on angle of attack are used to saturate the PI controller.

we call this curve the "winch control curve", though it is sometimes referred to as the "optimal force-squared speed manifold" [13].

3.2. Kite tether force control

The second system limit considered is a power limit. In steady-state, power equals tether force multiplied by reel-out speed, so the constant power lines appear as $1/x$ on the right plot in Fig. 3. It is assumed that the power limit is reached at the same reel-out speed as the tether force limit, as defined by the 2-phase strategy [19].

When the tether force and power limit are reached, the optimal strategy is to lower the lift-to-drag ratio of the kite to keep the tether force and reel-out speed constant and thus stay at the power limit. This is analogous to collective pitch control for wind turbines [14]. However, whereas in wind turbines, the generator speed is readily available as a feedback signal for the collective pitch controller, for airborne wind energy systems, the generator and kite are spatially separated. Thus, in this work, the tether force is used as a feedback signal, hence the name kite tether force control. The winch controller always stays on the $f^* = 1/3$ curve. This is to allow the tether force to go up so that the kite can use it as a feedback signal. This is contrary to wind turbine control, where constant torque or constant power torque control is typically used in region 3. The winch is thus responsible for keeping the system at the optimal reel-out speed, while the kite is responsible for staying below the tether force limit, and since the 2-phase strategy is used, limiting the tether force indirectly limits the power too.

The objectives of the kite angle of attack controller are thus twofold. First, when operating below the tether force limit, the kite shall fly at the optimum angle of attack, resulting in an optimal lift-to-drag ratio to extract the most power from the wind. Second, above the tether force limit, the kite must lower its angle of attack such that the system stays at the tether force limit. This shall be achieved with little overshoot above the reference tether force limit. Since the 2-phase strategy is used, this will also indirectly limit the power.

3.2.1. Controller design The proposed kite tether force controller uses a PI controller with anti-windup and dynamic inversion to calculate the angle of attack reference. The block diagram for this controller is shown in Fig. 4. The first part of the controller outputs a reference lift force for the kite based on the error between the reference and the actual tether force. In the second part of the controller, the reference lift force is used to calculate the reference angle of attack.

This is done using a linear lift curve, using

$$\alpha_{\text{ref}} = \frac{\frac{L_{\text{ref}}}{\frac{1}{2}\rho v_a^2 S} - C_{L_0}}{C_{L_\alpha}}, \tag{2}$$

where v_a denotes the (measured) airspeed, C_{L_0} the lift coefficient for 0 angle of attack, C_{L_α} the lift curve slope.

The PI controller uses a constant tether force reference, which is a little below the tether force limit to allow some margin for overshoot. When the system is above this reference, the PI controller will output a lower lift force reference, lowering the angle of attack reference. But when the system is operating below the tether force limit, the PI controller will increase the lift force reference to drive the angle of attack reference up to its optimal value, as desired. Back-calculation is used to avoid integrator wind-up and unsafe angle of attack references. Back-calculation limits the error going into the integrator, thus limiting the integral control action. It multiplies the difference between the saturated and unsaturated control signal (reference lift force in this case) by the back-calculation coefficient and subtracts it from the signal going into the integrator. In this work, $K_b = 1$ is used. The dynamic saturation comes from the minimum and maximum possible lift force the system can provide, based on the (fixed) minimum and maximum allowable angle of attack and the measured airspeed.

The proposed controller thus only uses a measurement of the tether force and airspeed, which can be obtained using a load sensor and pitot tube on the kite. Furthermore, its only model dependency is the linear lift curve, which is often known.

3.2.2. Tuning The two gains of the PI controller were tuned using a grid search where both gains are swept from 0 to 2.5 with a step size of 0.25. Some combinations of gains lead to failures in the simulation. These mostly occurred during the transition to the traction phase. Since this work does not focus on the retraction phase or transitions between phases, these failed simulations were disregarded.

Each simulation is evaluated on the following three control objectives.

(i) Low tether force overshoot to avoid tether rupture.
(ii) Low peak power to avoid generator overloading.
(iii) High mean power over the traction and retraction phase.

The results are shown in Fig. 5 and after a qualitative analysis with respect the control objectives, $K_\text{p} = 0.75$ and $K_\text{i} = 1.0$ were selected.

4. Results and discussion

In the following, three different control architectures will be compared:

(i) "baseline", proposed by [6] and discussed in Section 2, uses a winch controller that aims to keep the tether force constant without any power limit.
(ii) "optimal torque control" uses the different winch controller described in Section 3.1.
(iii) "kite tether force control", extends optimal torque control with a kite controller regulating the tether force to indirectly also regulate the power, as discussed in Section 3.2.

All simulations were run with a wind speed of 22 m/s to ensure that the power limit of the system is often reached and the effect of the kite tether force controller can be clearly shown. Furthermore, a steady wind field is used.

Fig. 6 shows the mechanical power output during the traction phase. With the baseline controller, power fluctuates between −5.8 MW and 20.5 MW every 12.5 seconds, or every half

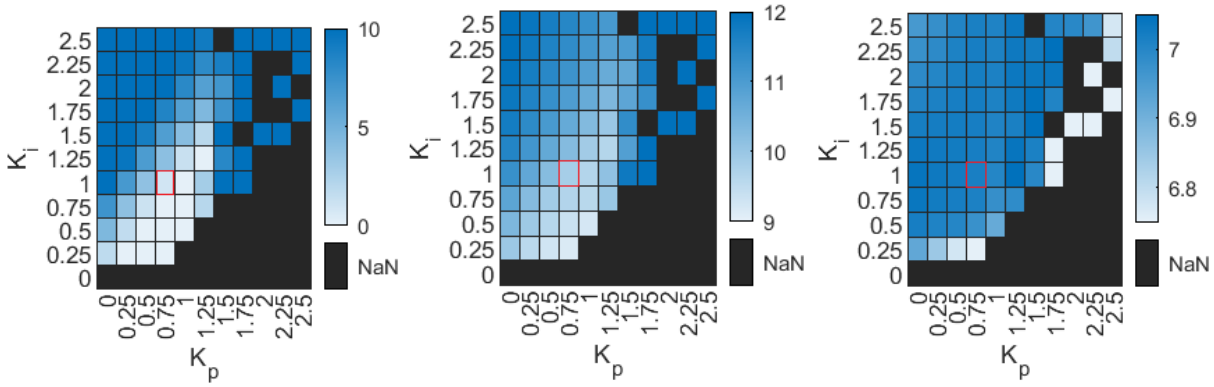

(a) Tether force overshoot [%] (b) Peak power [MW] (c) Mean power [MW]

Figure 5: Grid search for K_p and K_i with the selected values highlighted in red. Some combinations lead to failures, indicated by NaN.

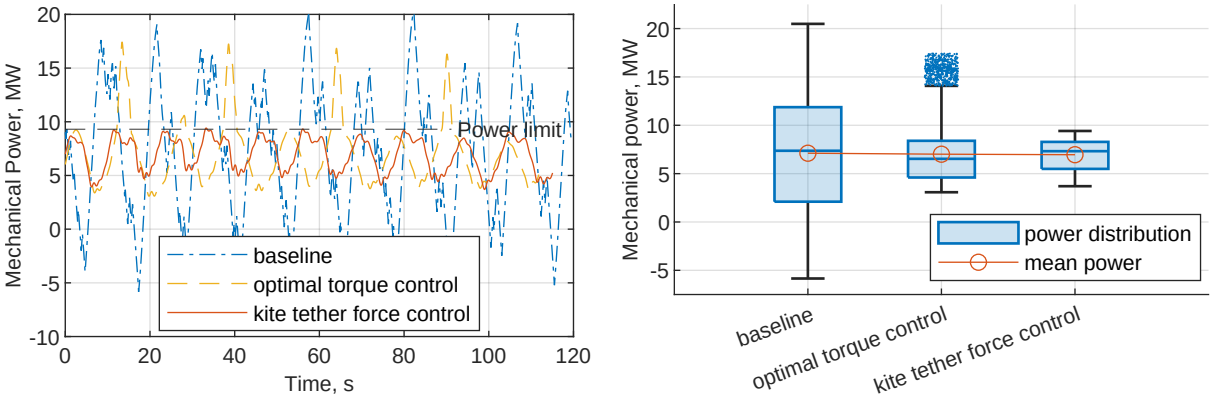

(a) (b)

Figure 6: Mechanical power output during the traction phase over time (a) and as boxplot together with mean power (b) (the dots around 15 MW for optimal torque control are outliers). The optimal torque controller increases the minimum power, while the kite tether force controller reduces the peak power. Together, they greatly reduce the power fluctuations.

figure of eight. High peak power occurs when gravity accelerates the kite during downward flight, while during upward flight more lift is spent overcoming gravity and the winch spends power to keep tether force constant. The optimal torque controller raises the minimum power to 3.1 MW. Introducing kite tether force control further reduces peak power to 9.4 MW. Overall, the range decreases by 75 %, when using the kite tether force control strategy.

Although the minimum and peak power output change significantly between the three control architectures, the mean power during the traction phase is minimally affected, as shown in Fig. 6b. The optimal torque controller produces 1.4 % less power, while the kite tether force controller produces 2.2 % less power. Nevertheless, the optimal torque controller (also used for the kite tether force controller) can be further optimized. As discussed in Section 3.1, the current winch controller is based on a quasi-steady model that neglects mass and uses an optimal reel-out factor of 1/3. In [13], the authors optimize the winch control curve for a relatively lightweight soft-wing ground system. A similar study could be done for MegAWES to optimize power production.

The mechanical output power is equal to the tether force multiplied by the reel-out speed

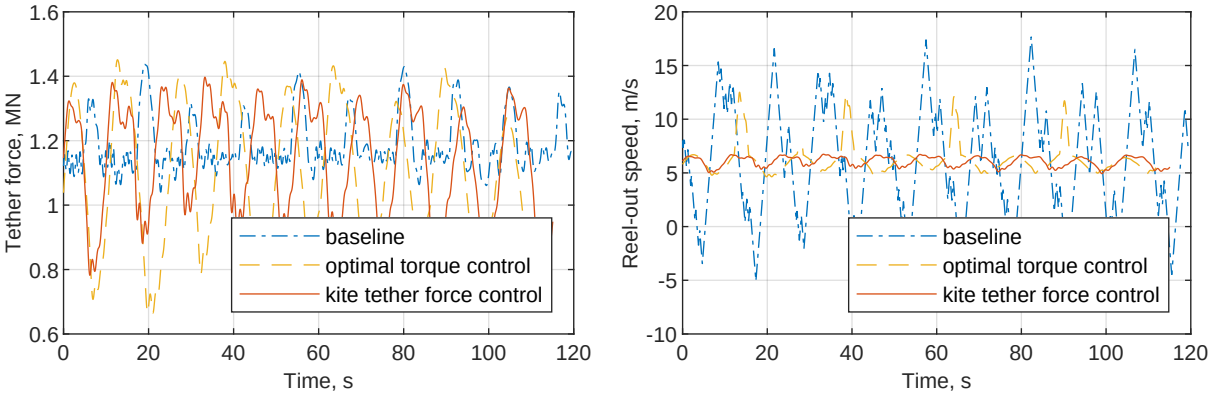

(a) Tether force. (b) Reel-out speed.

Figure 7: The optimal torque controller could increase the minimum power by allowing a lower tether force when the kite is flying upwards. However, it still had high peaks in reel-out speed to ensure the tether force did not exceed the limit. With the kite tether force controller, the peaks in reel-out speed are reduced, thus reducing the peak power.

when neglecting the acceleration of the winch (which has a small effect). So by looking at the tether force and reel-out speed, the cause for power smoothing can be analyzed. The baseline controller intermittently reels the kite in, consuming power to maintain a constant tether force, as evident in Fig. 7. The optimal torque controller goes to a lower tether force during low reel-out speeds, during upward flight. However, during downward flight, a high reel-out speed is still necessary to avoid overshooting the tether force limit. The kite tether force controller lowers the kite's angle of attack during these moments, reducing the peak power and smoothing the reel-out speed.

So the proposed control architecture reduces power oscillations but increases tether force fluctuations, now oscillating between 0.8×10^6 N and 1.4×10^6 N every 12.5 seconds. These fluctuations might give rise to new requirements on the system. Since they increase the fatigue damage on the tether, winch, and/or (floating) foundation. Furthermore, the system would likely reach lower tether forces at lower wind speeds, which might put the kite at risk of stalling. In [10], the authors propose a minimum torque for the winch, which ensures a minimum tether force to avoid this problem.

The kite's angle of attack is shown in Fig. 8. It is clear that when the tether force gets high, the kite starts flying at a lower angle of attack. Furthermore, when operating below the tether force limit (and thus below its power limit), the angle of attack is optimized for power extraction. While the angle of attack decreases every 12.5 seconds during the kite's downward flight, the lowest angle of attack varies between cycles. There are two observations to be made. First, there is an asymmetry between going down from the left or right side of the figure of eight. This correlates with an asymmetry in the airspeed and tracking error (not shown here), which is also present in the baseline. This is thus likely related to the lateral path loop. Second, the lowest angle of attack increases over time, but as previously seen in Fig. 7a, the peak tether force does not increase. This is explained by the tether drag. As the kite reels out, the tether drag increases, already lowering the lift-to-drag ratio of the kite-tether system. So the angle of attack must decrease less to reach the same lift-to-drag ratio that limits the tether force. This shows that the kite tether force controller is robust to changes in system dynamics arising from varying tether drag.

Besides winch and kite control, the flight path also contributes to power fluctuations. The figure of eight is flown outside-up, meaning that the kite has to overcome gravity when the cosine

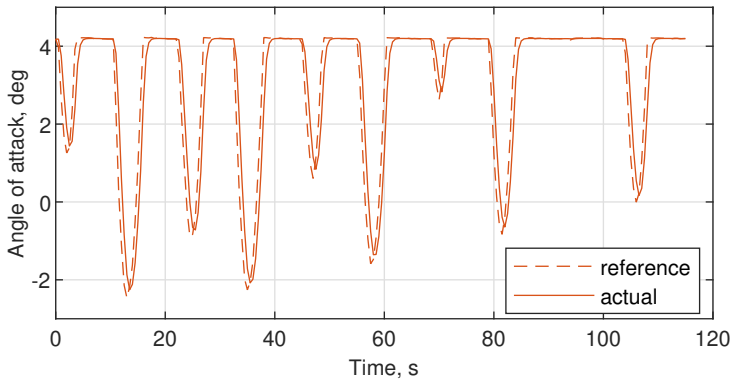

Figure 8: Angle of attack during the traction phase when using the kite tether force controller. It commands a lower angle of attack when the tether force would otherwise breach the limit.

losses [22] are the highest. In [23], the author suggests that using an outside-down flight path also lowers the power fluctuations. Especially at lower wind speeds, where the peak power is less likely to be reached, these other methods to achieve power smoothing might be necessary.

5. Conclusion

In this work, a new control architecture for MegAWES is proposed that uses an optimal torque winch controller and a novel kite tether force controller to achieve power smoothing at a wind speed of 22 m/s.

The optimal torque winch controller allows the system to operate at a lower tether force when the kite has to use more of its lift to counter gravity when flying upwards. This increased the minimum power from −5.8 MW to 3.1 MW, meaning that power consumption during the traction phase is eliminated.

To decrease the peak power, a novel kite tether force controller is proposed. It measures the tether force error and uses a PI controller with anti-wind to generate a lift force reference which is then transformed into an angle of attack reference using the linear lift curve and a measurement of the airspeed. It limits the peak tether force of the system, which indirectly limits the peak power since the 2-phase reeling strategy is used. This decreases the peak power from 20.5 MW to 9.4 MW, while only reducing mean power by 2.2 %. Together they thus reduce the range between minimum and maximum power by 75 %.

Now that the control architecture can take a power limit into account, future work can make a trade-off between the power limit and generator size for MegAWES, since a peak power of 9.4 MW might still be high for a rated power of 3.0 MW. Furthermore, the kite tether force controller can be combined with optimized paths, that further reduce power fluctuations, especially at lower wind speeds, where kite tether force control will be less active since the power limit might not be reached. Furthermore, it is apparent that there exists a trade-off between power fluctuations, which were present in the control architecture proposed by [6], and tether force fluctuations, present in this control architecture. Finally, the presented control architecture should also be tested on the 6DOF dynamics, where the kite will likely need good control authority over the angle of attack to follow the reference of the kite tether force controller.

References

[1] C. Vermillion, M. Cobb, L. Fagiano, R. Leuthold, M. Diehl, R. S. Smith, T. A. Wood, S. Rapp, R. Schmehl, D. Olinger and M. Demetriou 2021 *Annual Reviews in Control* **52** 330–357 DOI: 10.1016/j.arcontrol.2021.03.002

[2] M. L. Loyd 1980 *Journal of Energy* **4** 106–111 DOI: 10.2514/3.48021

[3] H. Schmidt, V. Leschinger, F. J. Müller, G. De Vries, R. J. Renes, R. Schmehl and G. Hübner 2024 *Energy Research & Social Science* **110** 103447 DOI: 10.1016/j.erss.2024.103447
[4] H. Schmidt, G. de Vries, R. J. Renes and R. Schmehl 2022 *Energies* **15** 1384 DOI: 10.3390/en15041384
[5] L. Fagiano, M. Quack, F. Bauer, L. Carnel and E. Oland 2022 *Annual Review of Control, Robotics, and Autonomous Systems* **5** 603–631 DOI: 10.1146/annurev-control-042820-124658
[6] D. Eijkelhof and R. Schmehl 2022 *Renewable Energy* **196** 137–150 DOI: 10.1016/j.renene.2022.06.094
[7] D. Eijkelhof, U. Fasel and S. Rapp 2021 MegAWES (3DoF & 6DoF kite dynamics) https://github.com/awegroup/MegAWES (Accessed: 2024-03-22)
[8] S. Rapp, R. Schmehl, E. Oland and T. Haas 2019 *Journal of Guidance, Control, and Dynamics* **42** 2456–2473 DOI: 10.2514/1.G004246
[9] R. Joshi, D. von Terzi, M. Kruijff and R. Schmehl 2022 *Journal of Physics: Conference Series* **2265** 042069 DOI: 10.1088/1742-6596/2265/4/042069
[10] A. U. Zgraggen, L. Fagiano and M. Morari 2016 *IEEE Transactions on Control Systems Technology* **24** 594–608 DOI: 10.1109/TCST.2015.2452230
[11] D. Todeschini, L. Fagiano, C. Micheli and A. Cattano 2021 *Control Engineering Practice* **111** DOI: 10.1016/j.conengprac.2021.104794
[12] M. Erhard and H. Strauch 2015 *Control Engineering Practice* **40** 13–26 DOI: 10.1016/j.conengprac.2015.03.001
[13] A. Berra and L. Fagiano 2021 An optimal reeling control strategy for pumping airborne wind energy systems without wind speed feedback *2021 European Control Conference (ECC)* (Delft, Netherlands: IEEE) pp 1199–1204 DOI: 10.23919/ECC54610.2021.9655018
[14] E. J. Novaes Menezes, A. M. Araújo and N. S. Bouchonneau Da Silva 2018 *Journal of Cleaner Production* **174** 945–953 DOI: 10.1016/j.jclepro.2017.10.297
[15] G. Licitra, J. Koenemann, A. Bürger, P. Williams, R. Ruiterkamp and M. Diehl 2019 *Energy* **173** 569–585 DOI: 10.1016/j.energy.2019.02.064
[16] J. De Schutter, R. Leuthold, T. Bronnenmeyer, R. Paelinck and M. Diehl 2019 Optimal control of stacked multi-kite systems for utility-scale airborne wind energy *2019 IEEE 58th Conference on Decision and Control (CDC)* (Nice, France: IEEE) pp 4865–4870 DOI: 10.1109/CDC40024.2019.9030026
[17] M. Zanon, S. Gros and M. Diehl 2013 Model Predictive Control of Rigid-Airfoil Airborne Wind Energy Systems *Airborne Wind Energy* Green Energy and Technology ed U. Ahrens, M. Diehl and R. Schmehl (Berlin, Heidelberg: Springer Berlin Heidelberg) pp 219–234 DOI: 10.1007/978-3-642-39965-7
[18] H. Li, D. J. Olinger and M. A. Demetriou 2015 Attitude tracking control of an Airborne Wind Energy system *2015 European Control Conference (ECC)* (Linz, Austria: IEEE) pp 1510–1515 DOI: 10.1109/ECC.2015.7330752
[19] R. H. Luchsinger 2013 Pumping Cycle Kite Power *Airborne Wind Energy* Green Energy and Technology ed U. Ahrens, M. Diehl and R. Schmehl (Berlin, Heidelberg: Springer Berlin Heidelberg) pp 47–64 DOI: 10.1007/978-3-642-39965-7_3
[20] J. Hummel, T. Pollack, D. Eijkelhof, E.-J. Van Kampen and R. Schmehl 2024 Winch Sizing for Ground-Generation Airborne Wind Energy Systems *2024 European Control Conference (ECC) (Accepted)* (Stockholm, Sweden)
[21] J. Hummel 2024 MegAWES - branch: DevTetherForceControl DOI: 10.4121/9dcf951c-753e-4b2c-ab89-4fab5a87d345
[22] M. Diehl 2013 Airborne Wind Energy: Basic Concepts and Physical Foundations *Airborne Wind Energy* Green Energy and Technology ed U. Ahrens, M. Diehl and R. Schmehl (Berlin, Heidelberg: Springer Berlin Heidelberg) pp 3–22 DOI: 10.1007/978-3-642-39965-7
[23] N. Rossi 2023 *Performance Comparison and Flight Controller of Circular and Figure-of-Eight Paths for Fixed-Wing Airborne Wind Energy System* MSc thesis University of Trento DOI: 10.5281/ZENODO.10160420